

# Large-Scale Magnetic Field Re-generation by Resonant MHD Wave Interactions

S. Galtier

Institut d'Astrophysique Spatiale (IAS), Bâtiment 121, F-91405 Orsay  
(France); Université Paris-Sud 11 and CNRS (UMR 8617)

and

S. Nazarenko

Mathematics Institute, The University of Warwick, Coventry, CV4-7AL,  
UK

## Abstract

We investigate numerically the long-time behavior of balanced Alfvén wave turbulence forced at intermediate scales. Whereas the usual constant-flux solution is found at the smallest scales, two new scalings are obtained at the forcing scales and at the largest scales of the system. In the latter case we show, in particular, that the spectrum evolves first to a state determined by Loitsyansky invariant and later a state close to the thermodynamic equipartition solution predicted by wave turbulence. The astrophysical implications for galactic magnetic field generation are discussed.

## 1 Introduction

Turbulence flows are ubiquitous in astrophysical environments from the solar wind (Goldstein et al., 1999; Galtier, 2006), to interstellar (Elergreen et al., 2004; Scalo et al., 2004), galactic and even intergalactic media (Govoni et al., 2006). At the larger scales, signatures of astrophysical turbulence are found, in particular, in the magnetic field measurements whose origin remains one of the major challenging problems (Pouquet, 1993; Widrow, 2002; Brandenburg, 2005). In this paper, we emphasize a new mechanism for generating large-scale magnetic field. It is based on the resonant interactions of shear-Alfvén waves in a turbulent medium permeated by a strong external magnetic field and influenced by an external forcing at intermediate scales. In this situation, both large-scale kinetic and magnetic energies may be produced by mainly non local interactions. This scenario, although very simple, may be

relevant for describing re-generation (i.e. maintenance) of large-scale galactic fields, e.g. in our galaxy where energy is injected at intermediate scales by stellar winds and supernovae explosions on scales 10 – 100pc (Ferriere et al., 2004).

## 2 Alfvénic turbulence

The wave kinetic equations of incompressible MHD were derived rigorously by Galtier et al. (2000,2002). Let us consider the simplest case when helicities are taken to be zero, when pseudo-Alfvén waves are discarded and when turbulence is axially symmetric and balanced (equal spectra for Alfvén waves co- and counter-propagating with respect to the external magnetic field). In this case for the shear-Alfvén wave energy spectrum we have  $E(k_{\perp}, k_{\parallel}) = f(k_{\parallel})E_{\perp}(k_{\perp})$ , where  $f(k_{\parallel})$  is a function fixed by the initial conditions (i.e. there is no energy transfer in the parallel direction), and the transverse part obeys the following kinetic equation, (Galtier et al., 2000)

$$\partial_t E_{\perp}(k_{\perp}) + \nu k_{\perp}^2 E_{\perp}(k_{\perp}) = \frac{\pi}{b_0} \int \cos^2 \phi \sin \theta \frac{k_{\perp}}{\kappa_{\perp}} E_{\perp}(\kappa_{\perp}) [k_{\perp} E_{\perp}(L_{\perp}) - L_{\perp} E_{\perp}(k_{\perp})] d\kappa_{\perp} dL_{\perp}. \quad (1)$$

Here  $b_0$  the background magnetic field (which will be taken equal to one),  $\phi$  the angle between  $\mathbf{k}_{\perp}$  and  $\mathbf{L}_{\perp}$ , and  $\theta$  the angle between  $\mathbf{k}_{\perp}$  and  $\kappa_{\perp}$ . This integro-differential equation has been computed in (Galtier et al., 2000) but only for short times in order to analysis, in particular, the formation of the Kolmogorov-Zakharov solution. In this paper we investigate the long-time behavior of Alfvén wave turbulence when of a forcing term is applied. In principle, this regime may be investigated for any value ( $\neq 1$ ) of the magnetic Prandtl number; in this case the viscosity  $\nu$  has to be seen as a combination of the kinematic viscosity and the magnetic diffusivity. Note that in the alfvénic turbulence regime, the kinetic and magnetic energies are equal, therefore all results may be interpreted in terms of magnetic energy fluctuations.

### 2.1 Short-time evolution

We perform numerical simulations of the wave kinetic equation (1) of MHD turbulence in which a forcing term is introduced at intermediate scales. A non-uniform grid in Fourier space is used (Galtier et al., 2000) with  $k_{\perp}(i) =$

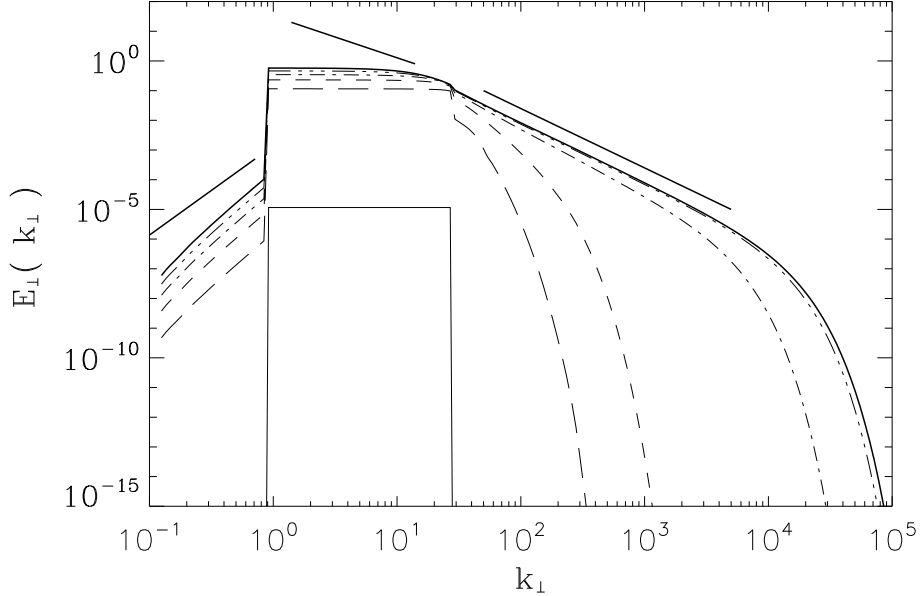


Figure 1: Evolution of the energy spectrum for times  $t_0 = 0$  (solid),  $t_1 = 5 \times 10^{-4}$  (long dash),  $t_2 = 2t_1$  (small dash),  $t_3 = 3t_1$  (dot-dash),  $t_4 = 4t_1$  (three dots-dash) and  $t_5 = 5t_1$  (bold solid). For comparison, three slopes are given with power law indices  $+3$ ,  $-1.4$  and  $-2$  respectively.

$\delta k \ 2^{i/F}$  ( $i \in [0, 156]$ ;  $\delta k = 1/8$ ;  $F = 8$ ). This method allows us to achieve very high Reynolds numbers ( $> 10^5$  with  $\nu = \eta = 5 \times 10^{-3}$ ). A weak forcing is applied to the flow at wavenumbers  $k_{\perp} \in [2^{-1/8}, 2^{19/4}]$  with a constant (flat) spectrum.

In Figure 1 the evolution of the shear-Alfvén wave energy spectrum is displayed for short times. The forcing scales determine the initial evolution as can be seen at intermediate wavenumbers. The first robust property to be observed is the generation of small-scales through a direct cascade and the formation of the well-know  $k_{\perp}^{-2}$  solution predicted by wave turbulence theory (Galtier et al., 2000). At the same time we see that the largest scales of the MHD flow are affected by the forcing and produce a power law slightly steeper than the reference slope ( $+3$ ). At intermediate scales, no clear tendency is observed yet, only a reduction of the flat spectrum seems to occur.

In Figure 2, we show the temporal evolution of the transfer function,

$T(k_\perp)$ , and the energy flux,  $P(k_\perp)$ , for the same times as in Figure 1. We remind the general relation in the inertial range (where forcing and dissipation are negligible)

$$\partial_t E_\perp = T = -\frac{\partial P}{\partial k_\perp}. \quad (2)$$

The constant flux solution of wave turbulence is clearly observed at small-scales and corresponds to a direct cascade (positive flux). As expected, a negative transfer is found at the forcing scales but a strong asymmetric profile is obtained initially which reduces with time. This reduction of asymmetry appears when the  $k_\perp^{-2}$  solution is well established (see Figure 1). At the largest scales a positive transfer with a negative (non constant) flux are found which means that energy is accumulated probably mostly by non-local interactions. Note that this is not an inverse cascade behaviour because there is no extra (in addition to the energy) positive invariant in our problem that could lead to a dual cascade process.

## 2.2 Intermediate-time evolution

In Figure 3, we show a next set of times that we call intermediate-time. Whereas the small-scale power-law spectrum appears to be stable with no apparent change, at the largest scales a  $k_\perp^3$  scaling is found. This solution could be related with the invariance of the Loitsyansky integral (Davidson, 2004; Bigot et al., 2007) which leads to scaling for the modal spectrum in  $k^{s-2}$  at low wavenumbers with  $s = D + 1$  ( $D$  being the space dimension). This analysis is often advocated to justify the scaling taken initially in (direct) numerical simulations. For example, it is shown in a recent work (Bigot et al., 2007) that the  $k_\perp^3$  scaling is well conserved in freely decaying wave MHD turbulence. At the intermediate scales, we see clearly a new scaling close to  $k_\perp^{-1.4}$ . It takes about one order of magnitude longer to build this solution than to form the small-scale cascade spectrum. We will see that this solution may be explained rigorously by an analysis based on the wave kinetic equation.

Figure 4 gives the transfer function and flux for the same times as in Figure 3. The constant flux at small-scale is still observed with an increase of its value in time; note that this increase seems to saturate. At wavenumbers around one, we see that the transfer function exhibits a change of sign going from a positive value, for wavenumbers smaller than one, to a negative value, for wavenumbers larger than one, which traduces an energy transfer towards

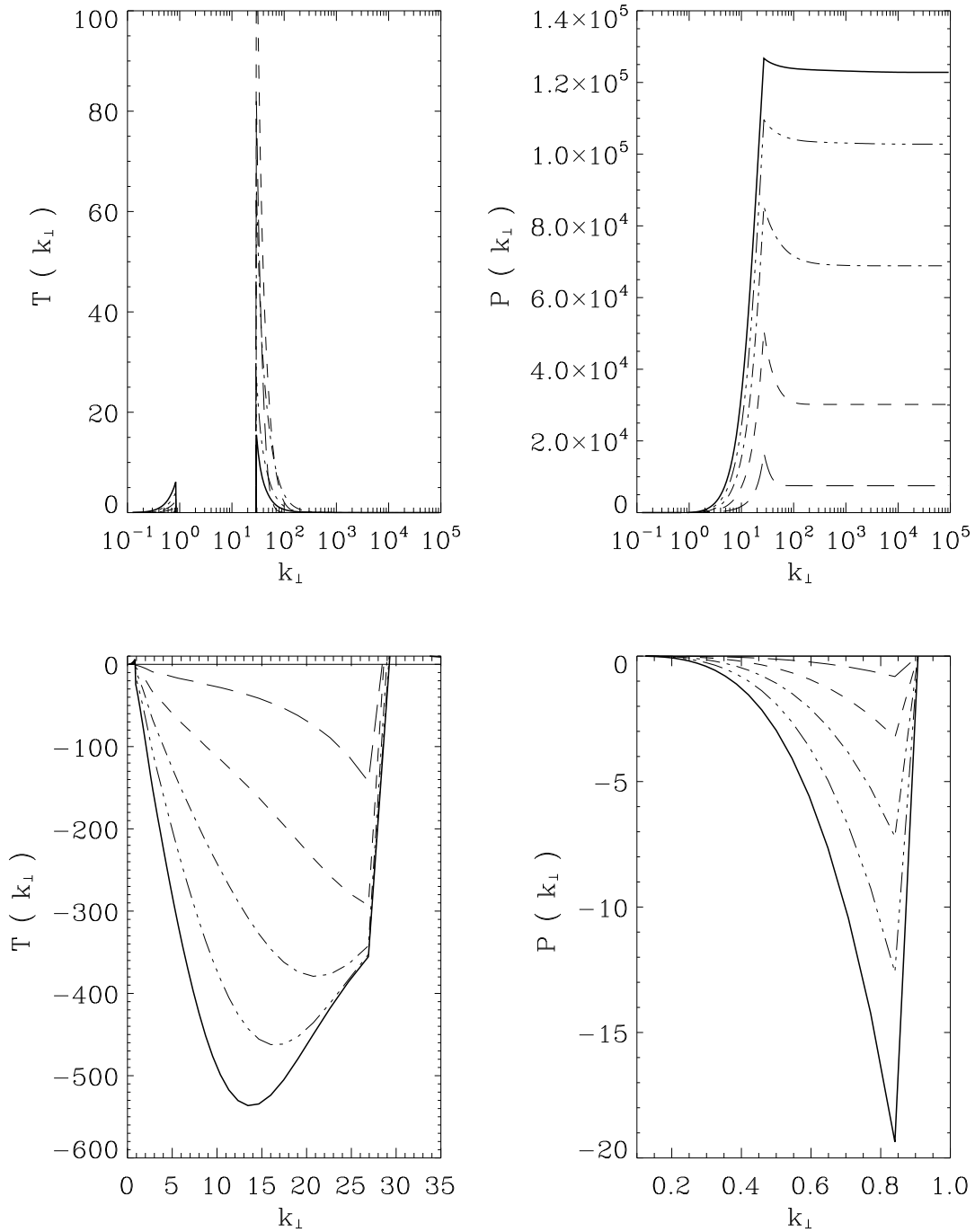


Figure 2: Temporal evolution of the transfer function  $T(k_{\perp})$  and the flux  $P(k_{\perp})$  at the same times as in Figure 1 (the same notation are also used). Top: general behavior at all scales of  $T$  and  $P$ ; note the formation of the constant flux solution at small-scales. Bottom: zoom at large-scales; a negative transfer is clearly seen at intermediate (forcing) scales whereas a negative flux is found at the largest scales.

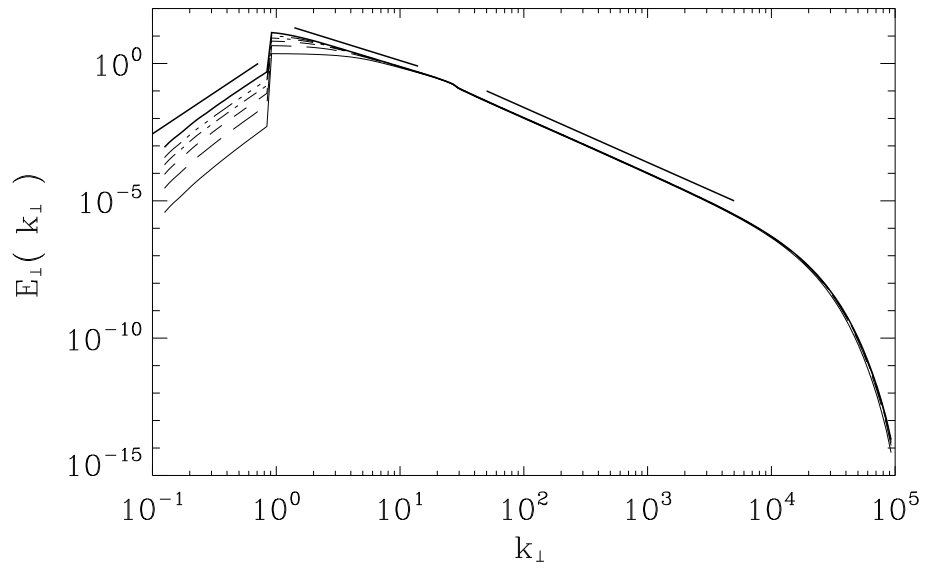


Figure 3: Evolution of the energy spectrum for times  $t_6 = 0.75 \times 10^{-2}$  (solid),  $t_7 = 1.75 \times 10^{-2}$  (long dash),  $t_8 = 2.75 \times 10^{-2}$  (small dash),  $t_9 = 3.75 \times 10^{-2}$  (dot-dash),  $t_{10} = 4.75 \times 10^{-2}$  (three dots-dash) and  $t_{11} = 0.1$  (bold solid). The same slopes as in Figure 1 are given.

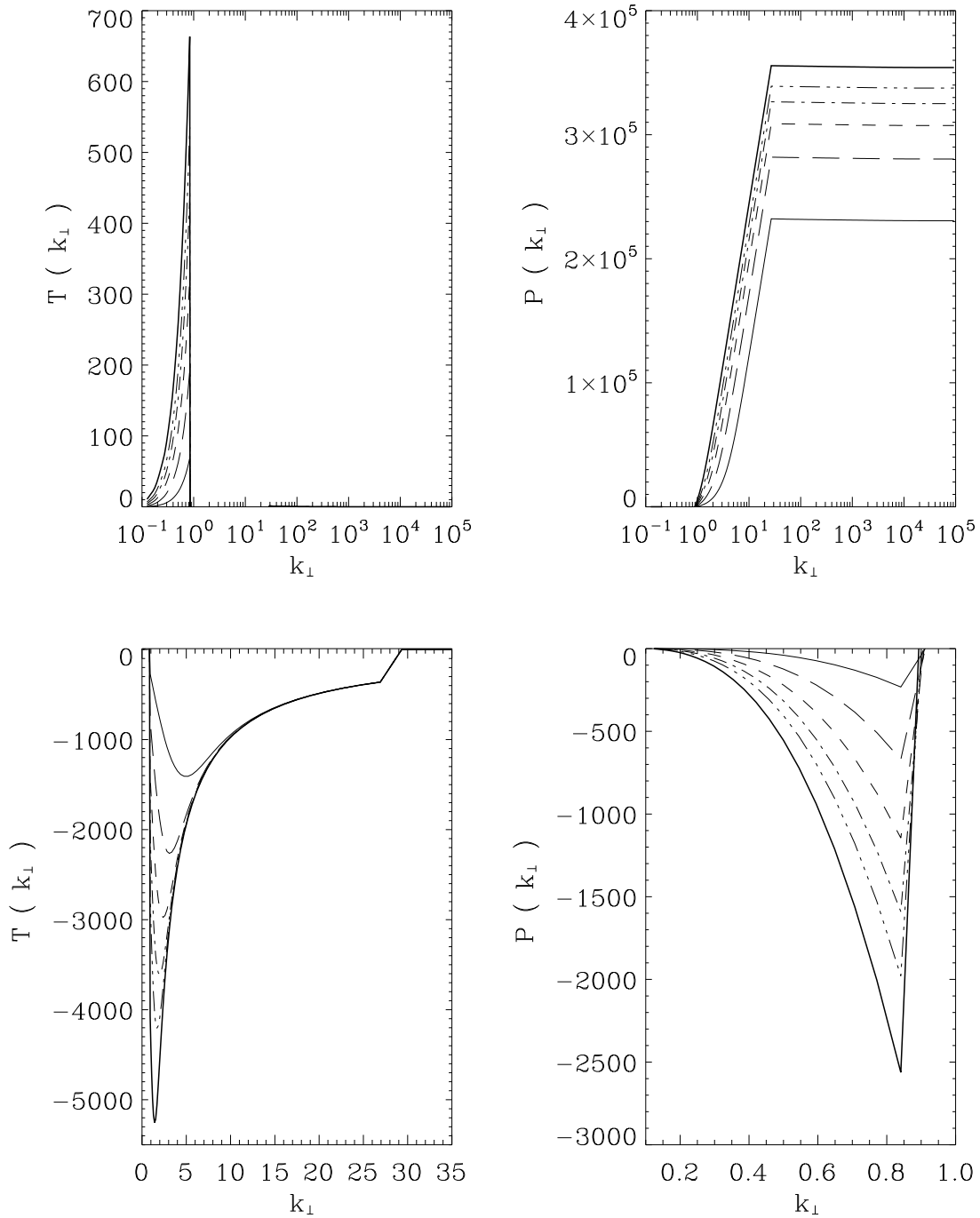


Figure 4: Temporal evolution of the transfer function  $T(k_{\perp})$  and the flux  $P(k_{\perp})$  at the same times as in Figure 3. Top: general behavior at all scales. Bottom: zoom at large-scale.

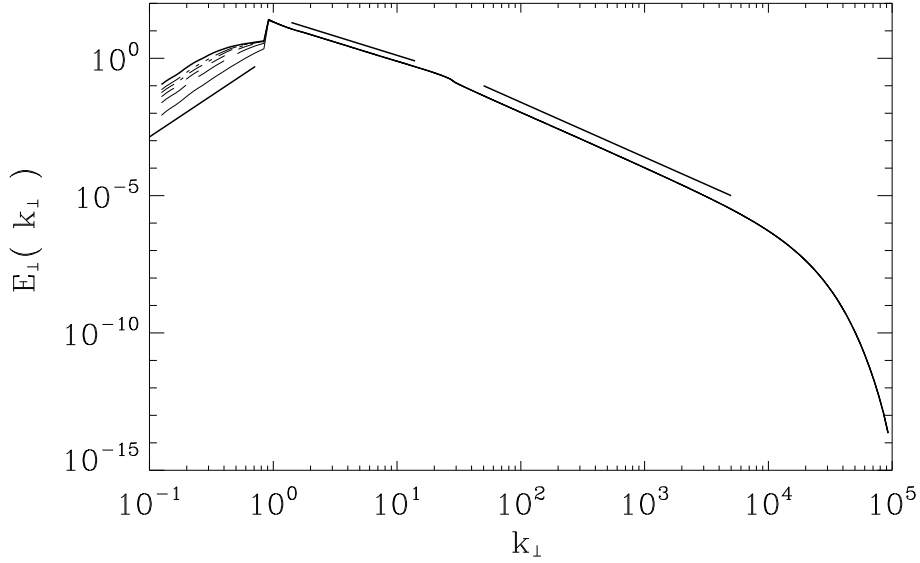


Figure 5: Long-time evolution of the energy spectrum at  $t_{12} = 0.15$  (solid),  $t_{13} = 0.35$  (long dash),  $t_{14} = 0.55$  (small dash),  $t_{15} = 0.75$  (dot-dash),  $t_{16} = 0.95$  (three dots-dash) and  $t_{17} = 1.45$  (bold solid).

larger scales. In the meantime, we note at the largest scales a decreasing of the flux which is still negative.

### 2.3 Asymptotically long-time evolution

The long-time behavior of Alfvén wave turbulence has been investigated as well. Figure 5 shows the energy spectrum evolution for times up to  $t = 1.45$ . Only the large-scale flow evolves at this stage, namely from the  $k_{\perp}^3$  scaling to a flatter power law.

Figure 6 gives more interesting information. The tendency to flux saturation observed at the smallest scales is confirmed and the transfer function at intermediates scale does not change anymore. As expected, only the largest scales are evolving with a transient decrease of the absolute value of the flux (which is negative at the large scales) accompanied by a plateau formation and a decrease of the transfer function.

The last set of graphs displays the final behavior (up to time  $t = 24.5$ ) of

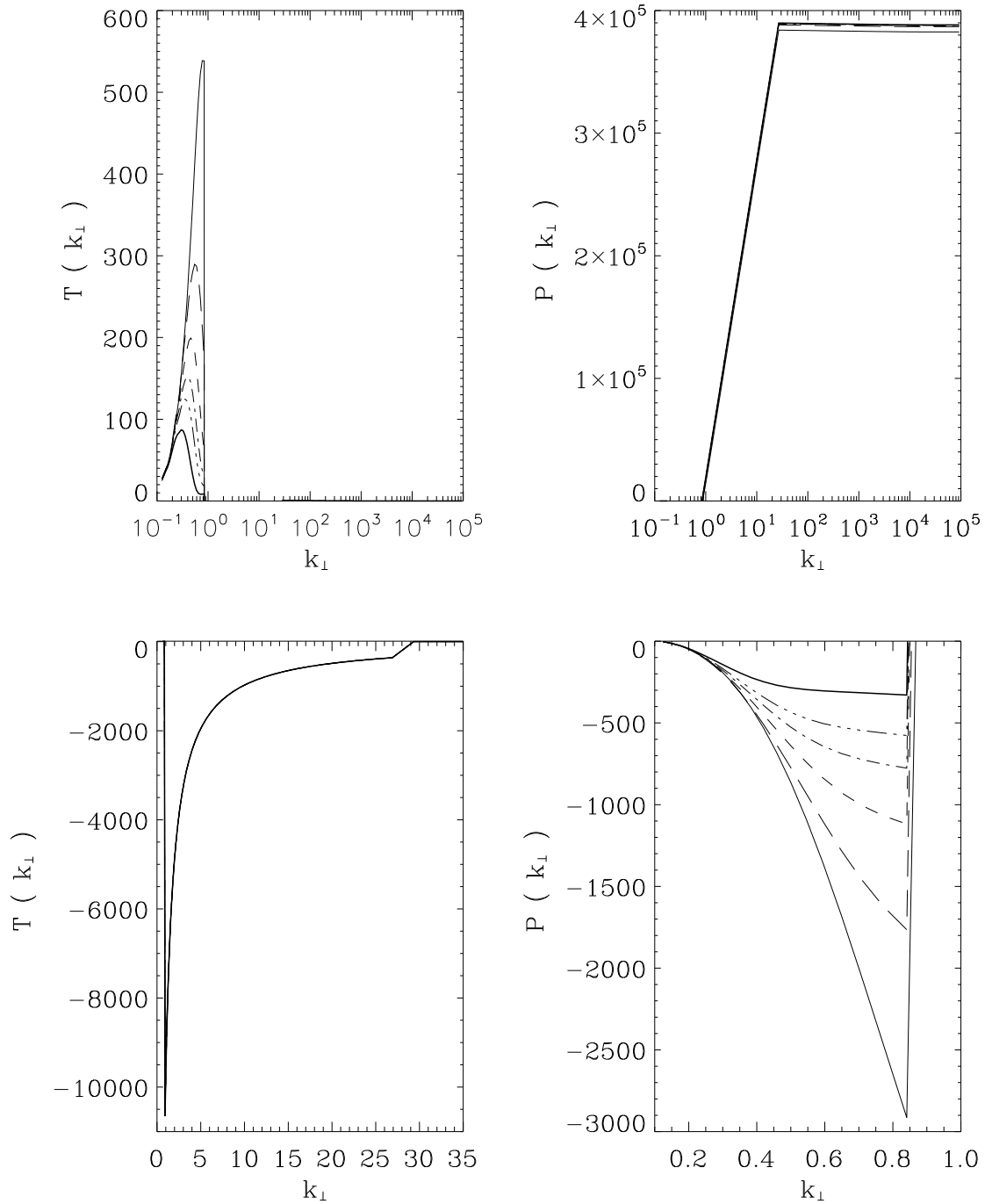


Figure 6: Temporal evolutions of the transfer function  $T(k_{\perp})$  and the flux  $P(k_{\perp})$  at the same times as in Figure 5.

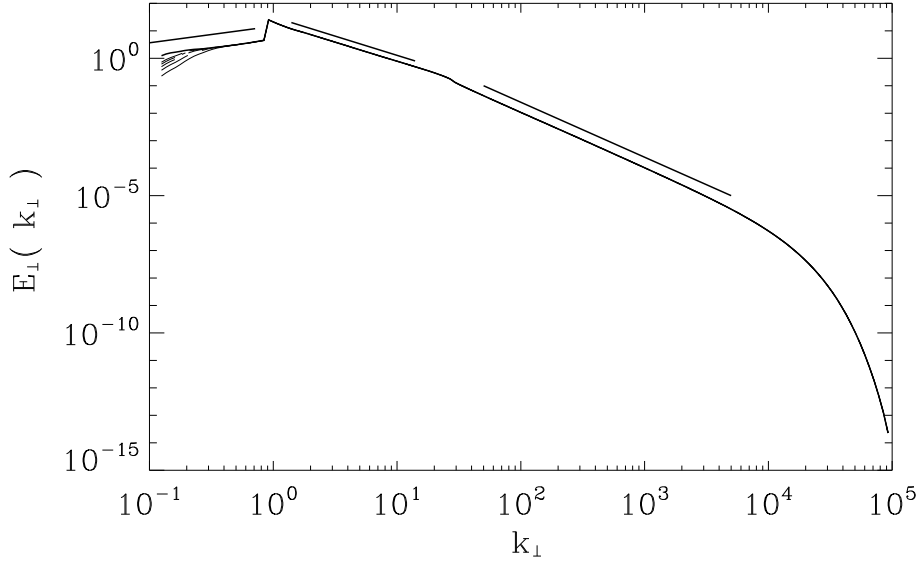


Figure 7: Asymptotically long-time evolution of energy spectrum at times  $t_{18} = 2.5$  (solid),  $t_{19} = 4.5$  (long dash),  $t_{20} = 6.5$  (small dash),  $t_{21} = 8.5$  (dot-dash),  $t_{22} = 10.5$  (three dots-dash) and  $t_{23} = 24.5$  (bold solid).

Alfvén wave turbulence. Figure 7 reveals the formation of a new power law close to  $k_{\perp}^{0.6}$  at the largest scales whereas the other scales are still steady.

In Figure 8 the flux weakening and the plateau formation is continuing at the largest scales whereas the transfer function is still decreasing.

### 3 Discussion

#### 3.1 Nonlinear dynamics at intermediate (forcing) scales

The scaling behavior found at intermediate scales seems to be strongly dependent on the type of forcing applied to the MHD flow. This is confirmed with a second simulation (not shown) where a non flat forcing is applied. The nonlinear dynamics at forcing scales may be investigated through a rigorous analysis based on the wave kinetic equations. Let us start from equation (1)

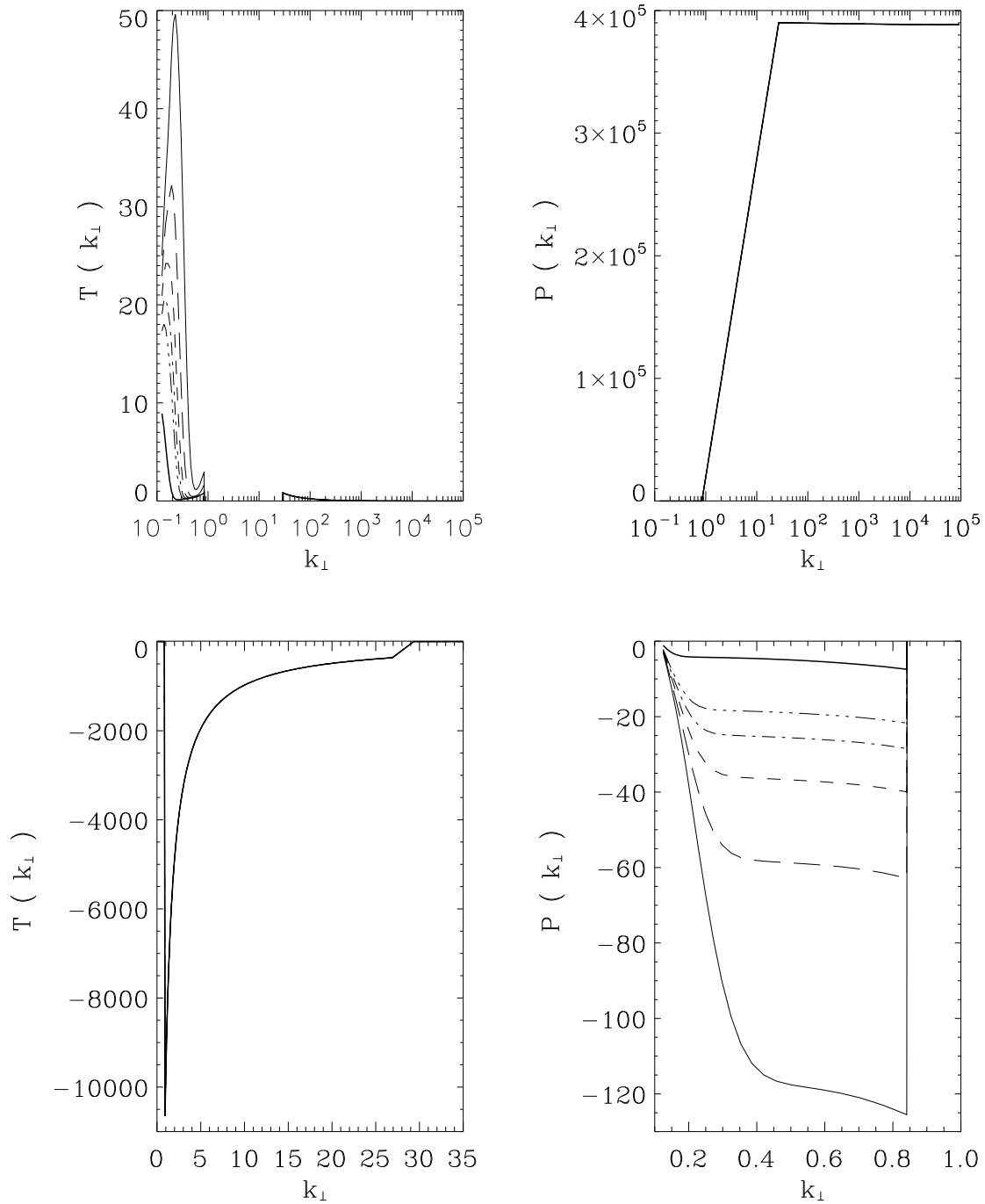


Figure 8: Temporal evolutions of the transfer function  $T(k_{\perp})$  and the flux  $P(k_{\perp})$  at the same times as in Figure 7.

and assume a power law scaling solution

$$E_{\perp}(k_{\perp}) = Ck_{\perp}^n. \quad (3)$$

Then let us assume the following general forcing

$$f(k_{\perp}) = C_f k_{\perp}^{\xi}. \quad (4)$$

Therefore, we have

$$\partial_t E_{\perp}(k_{\perp}) + \nu k_{\perp}^2 E_{\perp}(k_{\perp}) = C.I. + f(k_{\perp}), \quad (5)$$

where C.I. is the collision integral. We focus our analysis on the forcing scales and neglect the dissipative term. By introducing the notation  $\kappa_{\perp} = k_{\perp}x$  and  $L_{\perp} = k_{\perp}y$ , we obtain the steady solution

$$C^2 k_{\perp}^{2n+3} I(n) \sim C_f k_{\perp}^{\xi}, \quad (6)$$

where the collision integral writes

$$I(n) = \int_{\Delta} \left( \frac{y^2 + 1 - x^2}{2y} \right)^2 \sqrt{1 - \left( \frac{x^2 + 1 - y^2}{2x} \right)^2} x^{n-1} y (y^{n-1} - 1) dx dy. \quad (7)$$

Since  $I(n)$  is not singular, we directly obtain the scaling relation

$$n = \frac{\xi - 3}{2}. \quad (8)$$

For a constant (flat spectrum) forcing, we get  $n = -3/2$ . The solution found is indeed very close to this power law solution. The slight difference observed may be attributed to the non exact stationarity of the solution (see Figure 9). Note that we have tested the theoretical prediction against another forcing with  $\xi = 1$ . We find a steady energy spectrum in  $k_{\perp}^{-0.9}$  at intermediate scales which is close to the prediction in  $k_{\perp}^{-1}$  whereas the large-scale spectrum seems not to be affected and behaves similarly as in the simulation presented in this paper.

### 3.2 Solution at the largest scales

The asymptotically long-time evolution is characterized at the largest scales by a decreasing and flat in  $k$  energy flux (see Figure 8). Contrary to what

happens at the smallest scales, the flux has a very small value (around  $-5$  compare to  $4 \times 10^5$  at small scales) whereas the transfer function tends to zero. Therefore, the final state of Alfvén wave turbulence seems to be the zero-flux thermodynamic solution which corresponds to equipartition of energy in the  $k$ -space. In this case the theoretical solution derived in (Galtier et al., 2000) gives

$$E \sim k_{\perp}. \quad (9)$$

We see that the scaling found numerically is somewhat flatter, i.e.  $k_{\perp}^{0.6}$ . The difference may be attributed, in particular, to the limited time of computation which does not allow to reach exactly the zero-flux solution. The problem is that the evolution slows down dramatically as one moves closer to the lowest wavenumbers, and it takes an incredibly long computational time to reach the final state.

### 3.3 Global behavior

To complete our analysis, the temporal evolution of total shear-Alfvén wave energy is displayed in Figure 9 for times up to  $t = 2.5$ . Different time scalings are clearly visible: a first power law in  $t$  is found and a second in about  $t^{1/3}$  is estimated. The first temporal power law is linked to the formation of the Kolmogorov-Zakharov solution during which a transient solution with spectrum  $k_{\perp}^{-7/3}$  is produced (Galtier et al., 2000). The second temporal power law corresponds to the formation of the steady spectrum solution at intermediate scales discussed above. Finally, after time  $t > 0.2$  a plateau is reached with negligible energy variation in time (at least in logarithmic coordinate).

## 4 Conclusion

We have seen that the large-scale magnetic field is produced on a time-scale which is about  $10^4$  larger than the time-scale needed to establish the small-scale energy cascade solution. We believe that the final distribution in the large-scale part should correspond to the thermodynamic energy equipartition  $k_{\perp}^1$  even though it would take an extremely long computing time for formation of this spectrum which we were not able to achieve. Instead, we

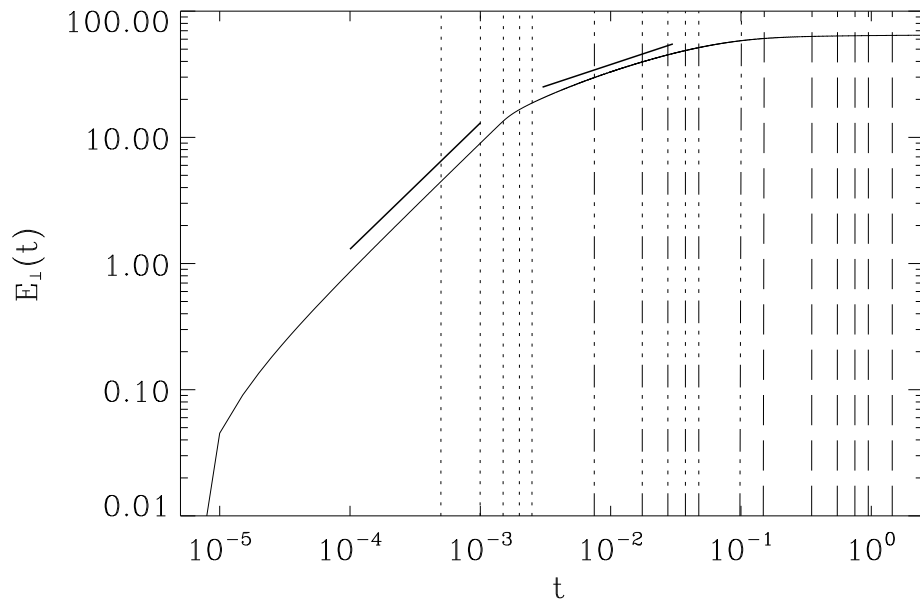


Figure 9: Temporal evolution of shear-Alfvén wave energy for times up to  $t_{18}$ . For comparison, two slopes are given with power law indices  $+1$  and  $+1/3$  respectively. The vertical lines correspond to times  $t_1$  to  $t_{17}$ .

observed formation of a shallower long-term scaling at the large scales,  $k_{\perp}^{0.6}$ , which we believe to be transient.

Because of the energy cascade to the smallest dissipative (resistive and viscous) scales, the small-scale part of the spectrum is important for understanding the total energy dissipation rate. On the other hand, it is this large-scale part of the spectrum that contains most of the wave (magnetic and kinetic) energy itself. One can view it as a sort of powerful energy storage which is charged extremely slowly and in a very inefficient way (because most of the charging energy is wasted via the energy cascade). For example, if the forcing is concentrated in a thin spherical shell with wavenumber lengths between  $k$  and  $k + \Delta k$  then the final energy at large scales (assuming the energy equipartition) will be  $k/\Delta k$  times greater than the energy at the forcing scales.

The mechanism of generation of large-scale magnetic fields via nonlinear transfer from an energy source at smaller scales may be relevant, in a very qualitative sense, to maintenance of large-scale galactic fields by small-scale sources provided by supernovae events. To pursue this line further, however, one would have to consider a more realistic thin disk geometry, instead of a simple homogeneous external field considered in the present paper, which could be an interesting future project.

## Acknowledgments

Grants from the PNST (Programme National Soleil–Terre) program of INSU (CNRS) are gratefully acknowledged.

## References

- [1] M.L. Goldstein and D.A. Roberts, 1999, Magnetohydrodynamics turbulence in the solar wind. *Phys. Plasmas* **6**, 4154–4160.
- [2] S. Galtier, 2006, Multi-Scale Turbulence in the Inner Solar Wind. *J. Low Temp. Phys.* **145**, 59–74.
- [3] B.G. Elmegreen and J. Scalo, 2004, Interstellar turbulence I: observations and processes. *Annu. Rev. Astron. Astrophys.* **42**, 211–273.

- [4] J. Scalo and B.G. Elmegreen, 2004, Interstellar turbulence II: implications and effects. *Annu. Rev. Astron. Astrophys.* **42**, 275–316.
- [5] F. Govoni, M. Murgia, L. Feretti, G. Giovanni, K. Dolag and G.B. Taylor, 2006, The intracluster magnetic field power spectrum in Abell 2255. *Astron. & Astrophys.* **460**, 425–438.
- [6] A. Pouquet, 1993, Magnetohydrodynamic turbulence. In *Astrophysical fluid dynamics* (ed. J.-P. Zahn and J. Zinn-Justin). Elsevier science publishers, 139–227.
- [7] L.M. Widrow, 2002, Origin of galactic and extragalactic magnetic fields. *Rev. Mod. Phys.* **74**, 775–823.
- [8] A. Brandenburg and K. Subramanian, 2005, Astrophysical magnetic fields and nonlinear dynamo theory. *Phys. Reports* **417**, 1–209.
- [9] J.L. Han, K. Ferriere and R.N. Manchester, 2004, The spatial energy spectrum of magnetic fields in our galaxy. *Astrophys. J.* **610**, 820-826.
- [10] S. Galtier, S.V. Nazarenko, A.C. Newell and A. Pouquet, 2000, A Weak Turbulence Theory for Incompressible MHD. *J. Plasma Phys.* **63**, 447–488.
- [11] S. Galtier, S.V. Nazarenko, A.C. Newell and A. Pouquet, 2002, Anisotropic Turbulence of Shear-Alfvén Waves. *Astrophys. J.* **564**, L49-L52.
- [12] S.V. Nazarenko, A.C. Newell and S. Galtier, 2001, Nonlocal MHD Turbulence. *Physica D* **152-153**, 646-652.
- [13] P.A. Davidson, 2004, Turbulence. Oxford University Press, New York.
- [14] B. Bigot, S. Galtier and H. Politano, 2007, Energy decay laws in strongly anisotropic MHD turbulence. Submitted to *Phys. Rev. Lett.*